

Non-dispersive graded impedance acoustic lenses

Sebastiano Cominelli*

Department of Mechanical Engineering, Politecnico di Milano, Milan, via La Masa 1, 20156 Milano, Italy

(Dated: January 3, 2025)

Lenses are typically based on refractive index profiles derived from the geometric approximation of high-frequency waves, yet the critical issue of impedance mismatch is often neglected. Mismatched devices suffer from unwanted reflections and dispersion, which can significantly degrade performance in practical applications. In this work, we propose impedance profiles for lenses to achieve efficient wave transmission while maintaining the desired refractive index and minimizing dispersion effects. A family of impedance profiles is derived from the acoustic wave equation such that the phase velocity is preserved. First, the 1D setting is considered to explain how dispersion occurs inside a lens and at its interfaces. Then, the method is applied to 2D axisymmetric configurations where the impedance mismatch is radially redistributed. These profiles are demonstrated in the acoustic setting of a Lüneburg lens, but can be easily extended to more general scenarios such as imaging or cloaking in air and water, where matching the impedance of the background poses significant challenges.

I. INTRODUCTION

Historically, lenses are developed using geometric optics, where wave propagation is approximated by ray trajectories that obey Snell's law. The simplest lenses consist of a homogeneous piece of dielectric whose geometry bends the rays at the interfaces with the background medium. More advanced lenses—such as the well-known Maxwell fisheye [1] and the Lüneburg lens [2]—rely on a spatially varying refractive index to manipulate a wave field. Following these pioneering works, novel index profiles for imaging have been continuously proposed [3–6]. This concept has recently been extended by the so-called transformation of coordinates, leading to more powerful devices such as concentrators, that focus waves within a target region [7], perfect lenses, enabled by negative index profiles [8, 9], and cloaking, which is emerging as one of the most striking applications [10–13].

The realization of such devices typically involves approximating the desired index profile with discrete material layers, called graded index (GRIN) materials. The advent of architected crystals has revolutionized this approach and extended graded index concepts to other fields, including acoustics. In this field, phononic crystals play a key role in providing the building blocks for acoustic devices [14].

Achieving a specific index profile does not require unique material properties, as it depends only on the wave speed, which is a function of, for example, dielectric permittivity and magnetic permeability in electromagnetism, or mass density and bulk modulus in acoustics. However, optimal performance is achieved when energy is efficiently transferred through the device, which occurs when the impedance of the device is matched to the surrounding medium. The challenge of impedance matching has been studied in several areas, such as electromagnetic

transmission lines [15], acoustic horns [16–18], and mechanical interfaces [19–21]. A key goal in these studies is to achieve near-perfect transmission over specific frequency intervals. In the one-dimensional (1D) setting, two media of different impedance are connected by a slab whose properties must be designed. Two well-established configurations allow efficient wave transmission: the quarter-wavelength constant impedance matching plate and the exponentially graded impedance [15, 19]. The latter represents the continuous limit of the former as the number of discrete matching layers increases [22]. In these scenarios, low-frequency waves are targeted as the signal wavelength is typically longer than the slab thickness, and the transmission characteristics from one side of the slab to the other are relevant. However, these studies are limited to 1D devices and do not take into account the phase distortion of the signal due to the device itself. The GRIN devices recently studied in the literature often interact with a signal for a few wavelengths [7, 23–29] because the wavelength is comparable to the device size. Working in such a mid-frequency range is necessary for several reasons, for example in order to exploit the low-frequency effective properties of a grating, or to allow the wave to interact with sensors that measure a spatial average of the wave field. In these scenarios, how the wave propagates within the device itself becomes important, and a constant impedance mismatch has been used in several contexts to preserve it. For example, in acoustics this strategy has been used to obtain a solid device that cloaks pressure waves in air [24, 30], and to design a cloak for water waves [31] to overcome the impossibility of changing the acceleration of gravity.

A constantly mismatched device directs a wave field through it as desired, but at the cost of reflections at the interface with the background. Then, in all of these settings, the impedance is as close as possible to the surrounding medium. Graded impedance has advantages. For example, a smooth transition with the surrounding medium can be achieved, reducing unwanted reflections, and the device properties can be modified more in the ar-

* sebastiano.cominelli@polimi.it

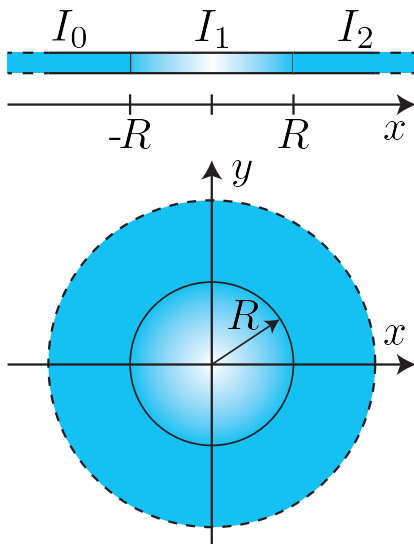


FIG. 1: Schematic of a 1D and a 2D lens with radius R .

cases where the realization is more critical. The drawback is that an impedance profile introduces dispersion, which affects wave transmission in the form of phase distortion. In this letter, we propose a method for changing the impedance of a device while preserving its index profile and its non-dispersive properties. The method is first introduced in the 1D scenario to get a close insight. We compute the reflection and transmission coefficients when the impedance has a non-continuous derivative and derive a formula that is more general than the canonical jump impedance transmission. An impedance profile without dispersion within the lens is derived. We extend the method to 2D axisymmetric devices where the mismatch is redistributed along the radius. The case of the Lüneburg lens is considered as an example. This approach facilitates practical implementation and reduces the drawbacks of a mismatched device for mid and high frequencies.

The paper focuses on the acoustic framework because it remains a challenge to mimic the impedance of typical acoustic media. For example, creating materials as light as air [24, 30, 32] or with the high bulk modulus of water [25–27, 33] is not trivial. Also, mass density and bulk modulus are usually adjusted independently when designing phononic crystals [27–29, 33, 34]. However, the theory is easily extended to other physical systems governed by similar mathematical structures, such as polarized electromagnetic waves or anti-plane elasticity, provided that the stiffness- and density-related terms can be tuned independently.

II. IMPROVED TRANSMISSION THROUGH GRADED MISMATCH

Consider the one-dimensional (1D) lens schematized in Figure 1, where the space is divided into three intervals $I_0 = (-\infty, -R)$, $I_1 = [-R, R]$, and $I_2 = (R, +\infty)$ along the x -axis, $R \in \mathbb{R}^+$. We assume constant properties in y and z directions and consider waves propagating only along x . The same homogeneous medium occupies I_0 and I_2 . Its mass density and bulk modulus are ρ_0 and K_0 , respectively. Conversely, the properties ρ_1 and K_1 of medium 1, the lens, are graded. The acoustic properties are typically also expressed in terms of acoustic impedance $Z_i := \sqrt{\rho_i K_i}$ and phase velocity $c_i := \sqrt{K_i/\rho_i}$. In this arrangement, a signal passing through the lens experiences amplitude and phase distortion according to the lens properties. Assuming a lens matched with the environment (i.e. $Z_1 = Z_0$), only a phase shift occurs due to the velocity profile defined as $n_1(x) := c_0/c_1(x)$, that is usually designed to achieve imaging—typically in 2D or 3D lenses. We look for a clever way to grade the impedance of the lens such that the phase shift is preserved as much as possible. For the sake of simplicity, we choose the most simple lens $n_1(x) \equiv 1$, but the method applies to the general case as discussed below for a 2D lens. Using the properties of medium 0 as reference, we write

$$\frac{K_0}{\rho_0} = \frac{K_1}{\rho_1}, \quad \frac{\rho_1}{\rho_0} = \frac{K_1}{K_0} = \frac{Z_1}{Z_0} = \alpha(x), \quad (1)$$

where $\alpha(x)$ is a bounded arbitrary function $\alpha: I_1 \rightarrow \mathbb{R}^+$ that grades the impedance in the medium 1.

The wave equation inside I_1 reads as

$$\left(\frac{1}{\alpha\rho_0}p_x\right)_x = \frac{1}{\alpha K_0}p_{tt}, \quad (2)$$

where the subscripts x and t indicates the partial derivatives in space and time, respectively. Given a graded impedance α , waves propagate differently through I_1 . To gain insight into the problem, we examine the well-known scenario of the exponentially graded impedance $\alpha_e = a_{0,e}e^{2a_{1,e}x}$ [19]. In this case, (2) admits solutions in the form

$$p_\alpha = e^{a_{1,e}x} \Re\{e^{j\omega t}(a_{2,e}e^{j\kappa(\omega)x} + a_{3,e}e^{-j\kappa(\omega)x})\}, \quad (3)$$

where the wavenumber $\kappa(\omega)$ satisfies the dispersion equation $\kappa^2 = \omega^2/c_0^2 - a_{1,e}^2$, and $a_{0,e}$, $a_{1,e}$, $a_{2,e}$, $a_{3,e} \in \mathbb{R}$ are arbitrary constants. j is the imaginary unit and \Re the real-part operator. The medium is clearly dispersive since the phase velocity is frequency dependent:

$$c(\omega) := \frac{\omega}{\kappa(\omega)} = c_0 \frac{\omega}{\sqrt{\omega^2 - a_{1,e}^2 c_0^2}}. \quad (4)$$

In addition, for $\omega < \omega_e := |a_{1,e}|c_0$ the wavenumber becomes purely imaginary, resulting in evanescent

waves. Thus, when the frequency is below ω_e , the graded medium does not efficiently transmit energy. This behavior can be qualitatively understood by considering that the wavelength at low-frequency is large compared to the spatial variation of the medium properties, and a continuous reflection occurs. Conversely, for high frequency ($\omega \gg \omega_e$) the reference sound speed c_0 is recovered.

When $\omega > \omega_e$, the exponential amplification $e^{a_1 x}$ in (3) is the effect of energy conservation of the wave. Indeed, the acoustic potential energy density is defined by $w = p^2/(2K)$, and for the right propagating wave of (3) it is

$$w(x, t) = \frac{a_{3,e}^2}{a_{0,e} 2K_0} \Re\{e^{j(\omega t - \kappa(\omega)x)}\}^2. \quad (5)$$

Thus, w propagates with the same speed of the wave.

A. Transmission without dispersion

If α is constant, Eq. (2) has the well-known solutions $p = p_1(x \pm c_0 t)$, representing backward and forward traveling waves with an arbitrary shape that is preserved during the propagation. Conversely, if the properties vary in space the shape of the wave changes due to energy conservation, as in the example shown above. In the general case of graded impedance α , we wonder whether there exists a property distribution that preserves the shape of any transmitted wave, even though the amplitude is gradually scaled as the wave propagates. To compute such an impedance profile, we look for a traveling wave in the form

$$p_\alpha = G(x, p_1(x - c_0 t)), \quad (6)$$

that is a wave propagating with speed c_0 and whose amplitude changes in space according to the function G . By substitution into Eq. (2) it yields:

$$\left[\left(\frac{1}{\alpha}\right)' G_x + \frac{1}{\alpha} G_{xx} \right] + \left[\frac{2}{\alpha} G_{xp} + \left(\frac{1}{\alpha}\right)' G_p \right] p_{1x} + \frac{G_{pp}}{\alpha} \left[(p_{1x})^2 - \frac{\rho_0}{K_0} (p_{1t})^2 \right] = 0, \quad (7)$$

where the identity (2) holding for p_1 has been used to simplify the equation. The subscripts x and p applied to G represent the partial derivatives with respect to the two explicit arguments of G , respectively, while the prime apex is the total derivative with respect to x . Eq. (7) is satisfied for all p_1 if its three terms cancel out independently:

$$\left(\frac{1}{\alpha}\right)' G_x + f G_{xx} = 0, \quad (8a)$$

$$\frac{2}{\alpha} G_{xp} + \left(\frac{1}{\alpha}\right)' G_p = 0, \quad (8b)$$

$$\frac{G_{pp}}{\alpha} = 0. \quad (8c)$$

Eq. (8c) implies $G_{pp} = 0$, then

$$G(x, p) = g(x)p + h(x) \quad (9)$$

for some functions g and h . This result is expected since it is the only possibility for G to preserve the linearity of the wave equation with respect to the pressure field. Substituting into (8a) and (8b) we obtain, respectively:

$$\left[\left(\frac{1}{\alpha}\right)' h' + \frac{h''}{\alpha} \right] + \left[\left(\frac{1}{\alpha}\right)' g' + \frac{g''}{\alpha} \right] \tilde{p}_1 = 0 \quad (10a)$$

$$2 \frac{g'}{\alpha} + \left(\frac{1}{\alpha}\right)' g = 0 \quad (10b)$$

that correspond to the three equations

$$\left(\frac{1}{\alpha}\right)' h' + \frac{h''}{\alpha} = 0, \quad (11a)$$

$$\left(\frac{1}{\alpha}\right)' g' + \frac{g''}{\alpha} = 0, \quad (11b)$$

$$2 \frac{g'}{\alpha} + \left(\frac{1}{\alpha}\right)' g = 0. \quad (11c)$$

This system of differential equations is solved to find α , g , and h up to integration constants. From (11a) and (11b):

$$\left(\frac{h'}{\alpha}\right)' = 0, \quad \left(\frac{g'}{\alpha}\right)' = 0. \quad (12)$$

Assuming $g \neq 0$, Eq. (11c) is equivalent to

$$\left(\frac{g^2}{\alpha}\right)' = 0. \quad (13)$$

Finally, the system is solved by

$$\alpha_{\text{nd}}(x) = a_{0,\text{nd}}(x + a_{1,\text{nd}})^{-2}, \quad (14a)$$

$$g(x) = a_{2,\text{nd}}(x + a_{1,\text{nd}})^{-1}, \quad (14b)$$

$$h(x) = a_{3,\text{nd}}(x + a_{1,\text{nd}})^{-1} + a_{4,\text{nd}}, \quad (14c)$$

for some constants $a_{i,\text{nd}}$, $i \in \{0, 1, 2, 3, 4\}$ that are determined by setting the problem and imposing the boundary conditions. Hence, a medium whose properties are graded as the non-dispersive profile (14a) sustains traveling waves of the type $p_\alpha = g(x)p_1(x \pm c_0 t) + h(x)$, for any function p_1 . Eq. (2) is invariant with respect to a pressure shift of h , just as is the homogeneous case for any first-order polynomial. Note that the homogeneous case is recovered when both α and g are constant (i.e. $a_{0,\text{nd}} \propto a_{1,\text{nd}}^2 \propto a_{2,\text{nd}}^2 \rightarrow \infty$).

A major result is that energy is transmitted efficiently for any frequency. Indeed, the acoustic potential energy density is

$$w(x, t) = \frac{g(x)^2}{\alpha_{\text{nd}}(x)} \frac{1}{2K_0} p_1(x \pm c_0 t)^2 = \frac{a_{2,\text{nd}}^2}{a_{0,\text{nd}}} w_0(x \pm c_0 t), \quad (15)$$

where w_0 is the energy of the field p_1 propagating in a homogeneous medium. w propagates with the same speed of the pressure wave, meaning that no dispersion occurs. Note that this property is a direct consequence of (13).

For the 1D lens, it is desired that symmetry with respect to $x = 0$ is preserved by the impedance grading. This is possible only if $a_{1,\text{nd}} = 0$ in (14a), i.e. $\alpha = a_{0,\text{nd}}x^{-2}$, leading to $\alpha(x \rightarrow 0) \rightarrow \infty$. To avoid this unfeasible choice, we define the function

$$\tilde{\alpha}_{\text{nd}}(x) := \begin{cases} \alpha_-(x) = a_{0,\text{nd}}(x - a_{1,\text{nd}})^{-2} & x < 0, \\ \alpha_+(x) = a_{0,\text{nd}}(x + a_{1,\text{nd}})^{-2} & x \geq 0. \end{cases} \quad (16)$$

So that the lens impedance is graded on both sides by a function of the form of (14a), at the cost of further reflections at $x = 0$ due to a slope discontinuity. A similar stratagem is required below to use the exponential profile.

B. Interface between two graded impedance media

Let us now consider what happens at the interface $x = 0$ inside medium 1, where the properties are graded by $\alpha_-(x) = \rho_-/\rho_0 = K_-/K_0$ for $x < 0$, and $\alpha_+(x) = \rho_+/\rho_0 = K_+/K_0$ for $x \geq 0$, respectively. If the profile given by (16) is adopted, $\alpha_-(-x) = \alpha_+(x)$, but they are kept independent the sake of generality. Given the functions α_- and α_+ in the form of (14a), the modulations g_- and g_+ are defined through (14b) up to arbitrary constants that we choose such that $g_-|_0 = g_+|_0 = 1$ —to uniquely define the reflected and transmitted amplitude. Using the time harmonic expansion, the pressure field at $x < 0$ is considered as the superposition of an incident wave $p_I = \Re\{g_-(x)e^{j(\omega t - \kappa x)}\}$ with unitary amplitude at the interface, and a reflected wave $p_R = \Re\{Rg_-(x)e^{j(\omega t + \kappa x)}\}$, with amplitude R . At $x \geq 0$, a right propagating wave is transmitted $p_T = \Re\{Tg_+(x)e^{j(\omega t - \kappa x)}\}$. ω is the angular frequency and $\kappa = \omega/c_0$ the wave number, that is the same on both sides since the sound speed is $c_- = c_+ = c_0$ everywhere and for every frequency. The continuity conditions read as

$$\begin{cases} (p_I + p_R)|_{0^-} = p_T|_{0^+} \\ \frac{1}{\rho_-}(p_I + p_R)_x|_{0^-} = \frac{1}{\rho_+}(p_T)_x|_{0^+} \end{cases} \quad (17)$$

By substitution, it yields

$$\begin{cases} T = \frac{2\kappa Z_+}{\kappa(Z_+ + Z_-) - j(Z_+g'_-|_0 - Z_-g'_+|_0)} \\ R = \frac{\kappa(Z_+ - Z_-) + j(Z_+g'_-|_0 - Z_-g'_+|_0)}{\kappa(Z_+ + Z_-) - j(Z_+g'_-|_0 - Z_-g'_+|_0)} \end{cases}, \quad (18)$$

where $Z_{\pm} = \alpha_{\pm}|_0 Z_0$. The classical formulae for T and R are recovered when the media are homogeneous, i.e. $g'_- = g'_+ = 0$. In the general scenario, reflections occur

$\alpha_c [-]$	$a_{0,e} [-]$	$a_{1,e} R [-]$	$f_e [Hz]$	$a_{0,\text{nd}} R^2 [-]$	$a_{1,\text{nd}} R [-]$
0.1	0.331	0.326	0.79	0.321	0.318
0.2	2.188	2.138	0.39	2.094	2.054

TABLE I: Coefficients of the impedance profiles.

for two reasons: (i) when there is an impedance mismatch ($Z_- \neq Z_+$), or (ii) when the wave changes shape ($g'_- \neq g'_+$). The latter phenomenon is frequency dependent, with reflections being stronger at lower frequencies. In the limit case, the zero frequency component experiences total reflection, with $T \rightarrow 0$ and $R \rightarrow -1$. Conversely, at high frequencies ($|\kappa/g'_-|_0|, |\kappa/g'_+|_0| \gg 1$), only the impedance mismatch at the interface dominates the transmission, giving $T \approx 2Z_+/(Z_+ + Z_-)$ and $R \approx (Z_+ - Z_-)/(Z_+ + Z_-)$, and total transmission occurs when $Z_- = Z_+$.

Nearby the interface, any impedance profile can be approximated in the form of (14a), so the formulae (18) extend to impedance profiles with a jump discontinuity and/or non-continuous derivative, when the refraction index is constant. In this case, we recall (13) about the interface and replace $g'_{\pm}|_0$ by $^{1/2}Z'_{\pm}/Z_{\pm}$, where $Z'_{\pm} := \alpha'_{\pm}|_0 Z_0$:

$$\begin{cases} T = \frac{2\kappa Z_+}{\kappa(Z_+ + Z_-) - j/2(Z_+Z'_-/Z_- - Z_-Z'_+/Z_+)} \\ R = \frac{\kappa(Z_+ - Z_-) + j/2(Z_+Z'_-/Z_- - Z_-Z'_+/Z_+)}{\kappa(Z_+ + Z_-) - j/2(Z_+Z'_-/Z_- - Z_-Z'_+/Z_+)} \end{cases} \quad (19)$$

To have a transmission that does not cause dispersion, one need to grade the impedance using a function in the form of (14a) and such that $Z'_- = Z'_+$ on any interface. It is easy to show that only a constant impedance meets both conditions. Therefore, any non-constant profile adopted to rescale the properties of the 1D lens introduces a frequency-dependent transmission either at the lens-background interfaces or within the lens itself. On top of that, multiple reflections inside the lens deteriorate the performance. To consider this, we numerically assess three profiles that reduce the mass of a lens: (i) the constant $\tilde{\alpha}_c(r) \equiv \alpha_c \in \mathbb{R}$, (ii) the exponential $\tilde{\alpha}_e := \alpha_e(|x|)$ and (iii) the non-dispersive $\tilde{\alpha}_{\text{nd}} := \alpha_{\text{nd}}(|x|)$, where the argument $|x|$ is the absolute value of x used to have a symmetric lens. The three profiles are chosen so that

$$\begin{cases} \tilde{\alpha}_{\text{nd}}(\pm R) = \tilde{\alpha}_e(\pm R) = 1 \\ \frac{1}{2R} \int_{-R}^R \tilde{\alpha}_{\text{nd}}(x) dx = \frac{1}{2R} \int_{-R}^R \tilde{\alpha}_e(x) dx = \alpha_c \end{cases}, \quad (20)$$

the former condition to match the impedance between the lens and the background, the latter to have the same mass of the lens among the three cases. We choose the two configurations $\alpha_c = 0.1$ and $\alpha_c = 0.2$, and get the coefficients shown in Table I and the mismatches shown in Figure 2a.

In the numerical simulation performed in COMSOL

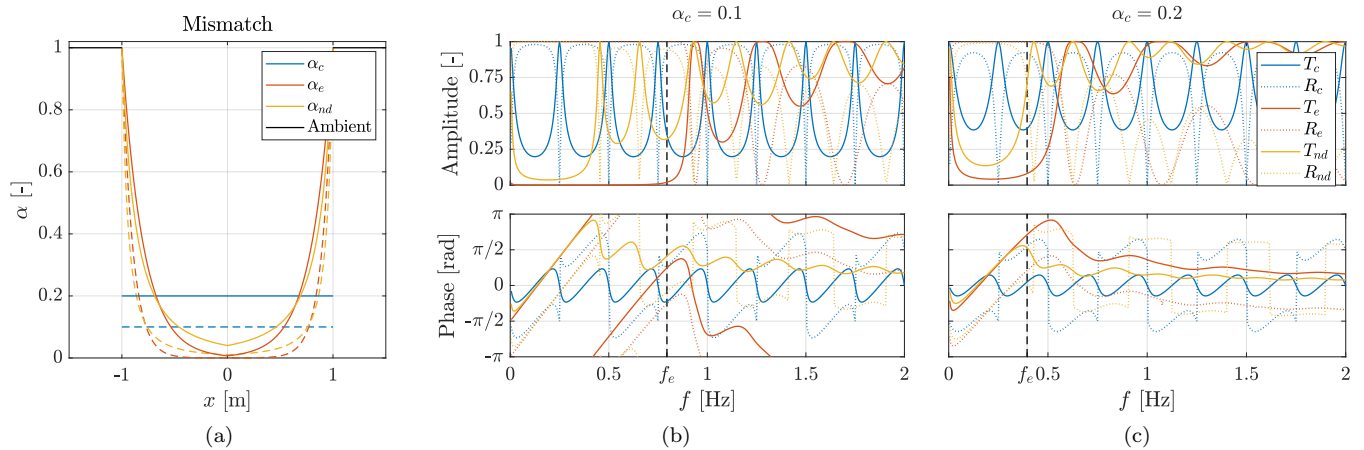


FIG. 2: The impedance profiles depicted in (a) are associated with the transmission and reflection coefficients shown in (b) for $\alpha_c = 0.1$ and in (c) for $\alpha_c = 0.2$.

Multiphysics[®], a harmonic wave of unitary amplitude is radiated from $-\infty$. The reflected and transmitted waves are measured at $x = \mp R$, respectively. Figure 2 shows the result in terms of amplitude and phase over the frequency range $f \in [0 \text{ Hz}, 2 \text{ Hz}]$, where $R = 1$ and $c_0 = 1$ have been chosen.

The constant mismatch has a frequency-periodic behavior, with perfect transmission at $f = \frac{nc_0}{4R}$, $\forall n \in \mathbb{N}$. Conversely, we distinguish three regions for the exponential and the non-dispersive profiles. At low frequency, both transmit a few energy because of the discontinuities at $x = \pm R$ and $x = 0$. In addition, the exponential profile transmit less below the minimum pass frequency $f_e := \frac{\omega_c}{2\pi}$. This also affects transmission at mid frequency, where the behavior is similar for both profiles. At high frequency, the amplitude T and R of both profiles tends to perfect transmission: $T \rightarrow 1$, $R \rightarrow 0$. The major difference is in the phase, where the non-dispersive profile performs better. These effects are accentuated when $\alpha_c = 0.1$, because f_e decreases further, as shown in Figure 2b.

III. LUNEBURG LENS WITH DISTRIBUTED MISMATCH

Let us now consider a 2D lens, where dispersion has a strong influence on the interference between waves traveling along different paths. In the following example, we also introduce a refractive index that varies along the radius, as is typical for circular lenses.

An impedance profile that limits dispersion is found by a similar procedure as before, for an axisymmetric lens with radius R and centered at the origin. Let $n(r)$ be the refractive index profile of the lens, where r is the distance from its center. Such a lens is perfectly matched if

$$\rho = \rho_0 n(r), \quad K = K_0/n(r), \quad (21)$$

so that $Z = Z_0$ everywhere. Note that ρ and K are bounded and non-null if n is bounded and non-null. Let $\alpha(r)$ be an arbitrary impedance profile along the radius, the wave equation for the mismatched lens reads as:

$$\nabla \cdot \left(\frac{1}{\alpha n \rho_0} \nabla p \right) = \frac{1}{\alpha n K_0} p_{tt}, \quad (22)$$

Let us assume that p_1 is the solution to (22) when $\alpha(r) \equiv 1$. We assume that the general the solution p_α has the form

$$p_\alpha = G(r, p_1), \quad (23)$$

where the function $G(r, p)$ explicitly depends on r and not on the tangential coordinate to enforce axial symmetry. Substituting p_α into (22) and repeating the same calculations as before but in polar coordinates, we obtain

$$G(r, p) = g(r) p + h(r) \quad (24a)$$

$$\alpha_{\text{nd}}(r) = a_{0,\text{nd}} (a_{1,\text{nd}} + N(r))^{-2} \quad (24b)$$

$$g(r) = a_{2,\text{nd}} (a_{1,\text{nd}} + N(r))^{-1} \quad (24c)$$

$$h(r) = a_{3,\text{nd}} (a_{1,\text{nd}} + N(r))^{-1} + a_{4,\text{nd}} \quad (24d)$$

for some constants $a_{i,\text{nd}}$, $i \in \{0, 1, 2, 3, 4\}$, and where $N(r) := \int_0^r n(\tilde{r})/\tilde{r} d\tilde{r}$. Then, for any choice of the five integration constants, the pressure field p_1 is modified without introducing material dispersion. The constant mismatch is recovered in the limit of $a_{0,\text{nd}} \propto a_{1,\text{nd}}^2 \rightarrow \infty$. Note that for $r \rightarrow 0^+$, N is unbounded if $n \neq 0$. This happens when the phase velocity is finite, as is typical for GRIN lenses. So $\alpha(r \rightarrow 0^+) = 0$ regardless of the values of a_0 and a_1 . This implies that vanishing properties are required in the center of the lens. This condition poses no issue when a sensor or an object must be placed at the center, as in sensing [5, 29] or cloaking [25, 35] devices. In cases where this is not feasible, introducing a

$\alpha_c [-]$	$a_{0,e} [-]$	$a_{1,e} R [-]$	$f_e [Hz]$	$a_{0,nd} [-]$	$a_{1,nd} [-]$
0.1	9.3×10^{-8}	16.2	1.29	6.7×10^{-3}	0.16
0.2	4.1×10^{-4}	7.80	0.62	4.1×10^{-2}	0.043

TABLE II: Coefficients of the 2D impedance profiles.

small void region at the center is sufficient to satisfy this requirement, at least in acoustic applications.

As an example, we consider the circular Lüneburg lens that focuses a set of parallel rays into one point on the external circumference [2]. The refraction index profile is

$$n_L(r) = \sqrt{2 - \frac{r^2}{R^2}}, \quad r \in [0, R] \quad (25)$$

The properties of the impedance-matched lens are defined according to (21). We aim to reduce the mass of the lens $m := \int_{\text{lens}} \rho dV$ while maintaining the imaging characteristics. The mass of the matched lens m_{ref} and its performance are taken as reference and three strategies are compared: (i) the constant impedance profile $\tilde{\alpha}_c \equiv \alpha_c \in \mathbb{R}$, (ii) the exponential profile $\tilde{\alpha}_e = a_{0,e} e^{a_{1,e} r}$, and (iii) the non-dispersive profile $\tilde{\alpha}_{\text{nd}} = a_{0,\text{nd}}(a_{1,\text{nd}} + N_L(r))^{-2}$, where

$$N_L(r) = n_L(r) + \sqrt{2} \operatorname{atanh} \left(n_L(r)/\sqrt{2} \right), \quad (26)$$

and atanh denotes the inverse of the hyperbolic tangent. The constants α_c , $a_{0,e}$, $a_{1,e}$, $a_{0,\text{nd}}$, $a_{1,\text{nd}}$ are defined such that

$$m_c = m_e = m_{\text{nd}} = \tilde{\alpha}_c m_{\text{ref}}, \quad (27a)$$

$$\alpha_e(R) = \alpha_{\text{nd}}(R) = 1. \quad (27b)$$

The former condition is such that the mass of the lens is reduced by the same amount $\tilde{\alpha}_c \in \{0.1, 0.2\}$; the latter requires the lens to match the background on the interface for α_e and α_{nd} . Eq. (27) is solved numerically to find the coefficients shown in Table II. The minimum frequency f_e of the exponential profile is calculated using the formula obtained in 1D to have a reference.

The performance of the impedance profiles is evaluated numerically. A plane wave of unitary amplitude propagating in the x direction is emitted from $(-\infty, 0)$ and focused by the lens at the point $F = (R, 0)$ on the outer surface of the lens. Figure 3 shows the pressure measured in F for the three configurations, normalized with respect to the measurement by the matched lens.

We note that the constant mismatch affects the wave

field similarly across the whole spectrum, while three distinct frequency regions can be identified for the exponential and non-dispersive profiles. At low frequencies, the smooth impedance profiles have a greater effect on performance than the constant profile. This is because at long wavelengths, the gradual transitions in material properties are perceived as a jump deeper than for a constant mismatch. At high frequencies, both exponential and non-dispersive impedance profiles do not noticeably change the performance of the lens because there are negligible reflections at the lens-background interface and dispersion within the lens. More importantly, in the mid-frequency range—where the wavelength is comparable to the size of the lens—the dispersion introduced by the exponential profile becomes significant, while the non-dispersive profile shows better performance.

IV. CONCLUSION

In this paper, we present a method for grading the impedance of lenses, providing a degree of freedom in their design. This approach is particularly valuable in scenarios where it is difficult to achieve material properties similar to those of the surrounding medium, as is often the case in acoustics. We discuss phase distortion and highlight that it generally occurs either at the device interfaces or within its volume. We quantify these two phenomena in the commonly used exponential profile and derive a generalized formula for the transmission and reflection problem. Our analysis shows that dispersion arises from abrupt changes in the slope of material properties. We construct a family of impedance profiles that prevent dispersion within a device, thereby improving its performance.

This approach is extended to 2D axisymmetric lenses where the impedance varies continuously along the radial direction. As an illustrative example, we apply the method to the design of a Lüneburg lens and demonstrate the practical potential of the approach. While the present work focuses on acoustics, the proposed method is broadly applicable to other physical systems governed by similar mathematical structures.

ACKNOWLEDGMENTS

I thank A. Cominelli for his insightful discussions that enriched this work.

-
- [1] W. Whewell, The Cambridge and Dublin Mathematical Journal **3**, Vol. 9 (E. Johnson, 1854).
 [2] R. K. Luneburg, Mathematical theory of optics (Univ of California Press, 1966).
 [3] J. C. Miñano, Perfect imaging in a homogeneous three-dimensional region, Optics express **14**, 9627 (2006).
 [4] S.-C. S. Lin, T. J. Huang, J.-H. Sun, and T.-T. Wu, Gradient-index phononic crystals, Physical Review B **79**,

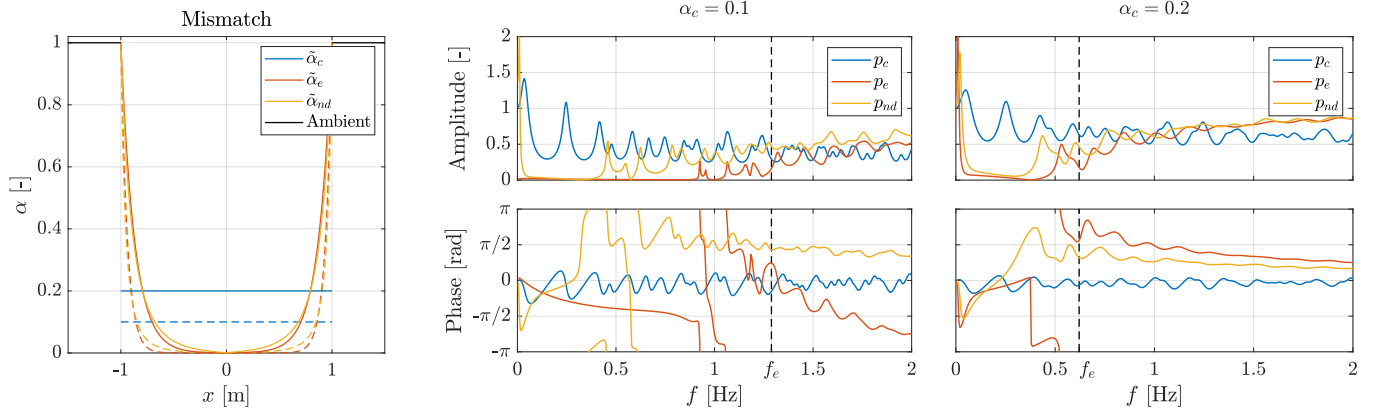


FIG. 3: The impedance profiles shown in (a) are associated with the pressure measured in (b) for $\alpha_c = 0.1$ and in (c) for $\alpha_c = 0.2$.

- 094302 (2009).
- [5] E. E. Narimanov and A. V. Kildishev, Optical black hole: Broadband omnidirectional light absorber, *Applied Physics Letters* **95** (2009).
- [6] X. Su, A. N. Norris, C. W. Cushing, M. R. Haberman, and P. S. Wilson, Broadband focusing of underwater sound using a transparent pentamode lens, *The Journal of the Acoustical Society of America* **141**, 4408 (2017).
- [7] M. Rahm, D. Schurig, D. A. Roberts, S. A. Cummer, D. R. Smith, and J. B. Pendry, Design of electromagnetic cloaks and concentrators using form-invariant coordinate transformations of maxwell's equations, *Photonics and Nanostructures-fundamentals and Applications* **6**, 87 (2008).
- [8] J. B. Pendry, Negative refraction makes a perfect lens, *Physical review letters* **85**, 3966 (2000).
- [9] S. A. Ramakrishna and J. Pendry, Spherical perfect lens: Solutions of maxwell's equations for spherical geometry, *Physical Review B* **69**, 115115 (2004).
- [10] J. B. Pendry, D. Schurig, and D. R. Smith, Controlling electromagnetic fields, *Science* **312**, 1780 (2006).
- [11] U. Leonhardt, Optical conformal mapping, *Science* **312**, 1777 (2006).
- [12] S. A. Cummer and D. Schurig, One path to acoustic cloaking, *New Journal of Physics* **9**, 45 (2007).
- [13] A. N. Norris, Acoustic cloaking theory, *Proceedings of the Royal Society A* **464**, 2411 (2008).
- [14] V. Laude, Phononic crystals: artificial crystals for sonic, acoustic, and elastic waves, *Landolt-Börnstein*, Vol. 26 (Walter de Gruyter GmbH & Co KG, 2015).
- [15] S. Ramo, J. R. Whinnery, and T. Van Duzer, *Fields and waves in communication electronics* (John Wiley & Sons, 1994).
- [16] A. G. Webster, Acoustical impedance and the theory of horns and of the phonograph, *Proceedings of the National Academy of Sciences* **5**, 275 (1919).
- [17] R. W. Klopfenstein, A transmission line taper of improved design, *Proceedings of the IRE* **44**, 31 (1956).
- [18] A. H. Benade and E. Jansson, On plane and spherical waves in horns with nonuniform flare: I. theory of radiation, resonance frequencies, and mode conversion, *Acta Acustica united with Acustica* **31**, 79 (1974).
- [19] P. C. Pedersen, O. Tretiak, and P. He, Impedance-matching properties of an inhomogeneous matching layer with continuously changing acoustic impedance, *The Journal of the Acoustical Society of America* **72**, 327 (1982).
- [20] Z. Li, D.-Q. Yang, S.-L. Liu, S.-Y. Yu, M.-H. Lu, J. Zhu, S.-T. Zhang, M.-W. Zhu, X.-S. Guo, H.-D. Wu, et al., Broadband gradient impedance matching using an acoustic metamaterial for ultrasonic transducers, *Scientific reports* **7**, 42863 (2017).
- [21] D. Hui and P. K. Dutta, A new concept of shock mitigation by impedance-graded materials, *Composites Part B: Engineering* **42**, 2181 (2011).
- [22] G. Kossoff, The effects of backing and matching on the performance of piezoelectric ceramic transducers, *IEEE Transactions on sonics and ultrasonics* **13**, 20 (1966).
- [23] W. Cai, U. K. Chettiar, A. V. Kildishev, and V. M. Shalaev, Optical cloaking with metamaterials, *Nature photonics* **1**, 224 (2007).
- [24] B.-I. Popa, L. Zigoneanu, and S. A. Cummer, Experimental acoustic ground cloak in air, *Phys. Rev. Lett.* **106**, 253901 (2011).
- [25] D. E. Quadrelli, M. A. Casieri, G. Cazzulani, S. La Riviera, and F. Braghin, Experimental validation of a broadband pentamode elliptical-shaped cloak for underwater acoustics, *Extreme Mechanics Letters* , 101526 (2021).
- [26] Y. Bi, H. Jia, Z. Sun, Y. Yang, H. Zhao, and J. Yang, Experimental demonstration of three-dimensional broadband underwater acoustic carpet cloak, *Applied Physics Letters* **112**, 233502 (2018).
- [27] Q. Li and J. S. Vipperman, Three-dimensional pentamode acoustic metamaterials with hexagonal unit cells, *The Journal of the Acoustical Society of America* **145**, 1372 (2019).
- [28] S. Cominelli, D. E. Quadrelli, C. Sinigaglia, and F. Braghin, Design of arbitrarily shaped acoustic cloaks through partial differential equation-constrained optimization satisfying sonic-metamaterial design requirements, *Proceedings of the Royal Society A* **478**, 20210750 (2022).
- [29] S. Cominelli and F. Braghin, Optimal design of broadband, low-directivity graded index acoustic lenses for underwater communication, *The Journal of the Acoustical Society of America* **156**, 1952 (2024).

- [30] L. Zigoneanu, B.-I. Popa, and S. A. Cummer, Three-dimensional broadband omnidirectional acoustic ground cloak, *Nature materials* **13**, 352 (2014).
- [31] G. Dupont, S. Guenneau, O. Kimmoun, B. Molin, and S. Enoch, Cloaking a vertical cylinder via homogenization in the mild-slope equation, *Journal of Fluid Mechanics* **796**, R1 (2016).
- [32] W. Kan, V. M. García-Chocano, F. Cervera, B. Liang, X.-y. Zou, L.-l. Yin, J. Cheng, and J. Sánchez-Dehesa, Broadband acoustic cloaking within an arbitrary hard cavity, *Physical Review Applied* **3**, 064019 (2015).
- [33] G. Brambilla, S. Cominelli, M. Verbicaro, G. Cazzulani, and F. Braghin, High bulk modulus pentamodes: The three-dimensional metal water, *Extreme Mechanics Letters* , 102267 (2024).
- [34] M. Kadic, T. Bückmann, R. Schittny, P. Gumbsch, and M. Wegener, Pentamode metamaterials with independently tailored bulk modulus and mass density, *Physical Review Applied* **2**, 054007 (2014).
- [35] Y. Chen, M. Zheng, X. Liu, Y. Bi, Z. Sun, P. Xiang, J. Yang, and G. Hu, Broadband solid cloak for underwater acoustics, *Physical Review B* **95**, 180104 (2017).